Neutrino textures and charged lepton flavor violation in light of θ_{13}, MEG, and LHC data

M. Cannoni,[1] J. Ellis,[2,3] M. E. Gómez,[1] and S. Lola[4]

[1]*Department of Applied Physics, University of Huelva, 21071 Huelva, Spain*
[2]*Department of Physics, Theoretical Particle Physics and Cosmology Group, King's College London, Strand, London WC2R 2LS, United Kingdom*
[3]*Physics Department, Theory Division, CERN, CH-1211 Geneva 23, Switzerland*
[4]*Department of Physics, University of Patras, 26500 Patras, Greece*

(Received 2 August 2013; published 9 October 2013)

In light of recent results from the LHC, MEG and neutrino experiments, we revisit the issue of charged lepton flavor violation (LFV) in supersymmetric theories with massive neutrinos, where flavor-violating soft supersymmetry-breaking masses for sleptons are induced naturally by radiative corrections. We link our results to the expectations for light neutrinos with a normal mass hierarchy in SU(5), enhanced by an Abelian flavor symmetry, with particular focus on θ_{13}. We focus on the radiative decays $\ell_i \to \ell_j \gamma$ and on detection prospects at the LHC and a linear collider (LC). We use supersymmetric parameters consistent with cosmological considerations and with LHC searches for supersymmetry and the Higgs mass. We find a class of scenarios where the LHC may be sensitive to LFV sparticle decays and LFV processes could be detectable at a LC with center-of-mass energy above 1 TeV, whereas LFV lepton decays may be suppressed by cancellations in the decay amplitudes.

DOI: 10.1103/PhysRevD.88.075005 PACS numbers: 12.60.Jv, 14.60.Pq, 11.30.Hv

I. INTRODUCTION

In recent years, the existence of neutrino masses and oscillations with near-maximal $\nu_\mu - \nu_\tau$ and large $\nu_e \to \nu_\mu$ mixing has been established by extensive input from atmospheric [1], solar [2] and long-baseline reactor [3] and accelerator [4,5] neutrino experiments. Initial input on the possible range of the θ_{13} [6,7] was provided by the T2K [8] and MINOS Collaborations [9], and definitive evidence for a nonzero value of θ_{13} has been provided by the reactor experiments Daya Bay [10] and RENO [11], and very recently also by Double Chooz [12].

A natural expectation in theories with massive neutrinos is charged lepton flavor violation (LFV), which is enhanced in supersymmetric theories via the renormalization of soft supersymmetry-breaking parameters. The link between neutrino oscillations and violations of the individual lepton numbers $L_{e,\mu,\tau}$ raises the prospect of observing processes such as $\mu \to e\gamma$, $\mu \to 3e$, $\tau \to \mu\gamma$ and $\mu \to e$ conversion on heavy nuclei [13]. The present experimental upper limits on the most interesting of these processes, summarized below, already constrain significantly the parameter spaces of theoretical models [14,15]:

$$\mathrm{BR}(\mu \to e\gamma) < 5.6 \times 10^{-13}, \tag{1}$$

$$\mathrm{BR}(\tau \to \mu\gamma) < 4.4 \times 10^{-8}, \tag{2}$$

$$\mathrm{BR}(\tau \to e\gamma) < 3.3 \times 10^{-8}, \tag{3}$$

The strongest constrain on radiative decays is the recent upper limit on $\mathrm{BR}(\mu \to e\gamma)$ [14] from the MEG experiment, 4 times more stringent than the previous one [16].

Within the supersymmetric framework, one should also keep in mind other possibilities for observing LFV processes, such as slepton pair production at a linear collider (LC) [17–24] and signals at the LHC [25–32], particularly in $\chi_2 \to \chi + e^{\pm}\mu^{\mp}$ $\chi_2 \to \chi + \mu^{\pm}\tau^{\mp}$ decays [here χ is the lightest neutralino, assumed to be the lightest supersymmetric particle (LSP), and χ_2 is the second-lightest neutralino]. These decays could provide search prospects that are complementary to direct searches for flavor-violating decays of charged leptons, particularly for heavy superparticle spectra.

In this paper we reevaluate the prospects for observable charged LFV, based on updated knowledge of neutrino mass and mixing parameters that includes the recent measurement of θ_{13}. We work within the framework of the most natural mechanism for obtaining hierarchical light neutrino masses, namely the seesaw mechanism [33], in which an effective Majorana mass matrix for light neutrinos, $m_{\mathrm{eff}} = m_\nu^D \cdot (M_N)^{-1} \cdot m_\nu^{D^T}$, arises from Dirac neutrino masses m_ν^D of the same order as the charged lepton and quark masses, and heavy Majorana masses M_N. In supersymmetric theories, the neutrino Dirac couplings Y_ν renormalize the soft supersymmetry-breaking sneutrino and slepton masses, generating LFV in a natural way [34]. Even if the soft scalar masses were universal at the unification scale, quantum corrections between the grand unified theory (GUT) scale and low energies would modify this structure via renormalization-group running, which generates off-diagonal contributions. This effect is particularly interesting in seesaw models, where in general the Dirac neutrino Yukawa couplings cannot be diagonalized

simultaneously with the charged lepton and slepton mass matrices [34]. Given the large mixing of the corresponding neutrino species, charged LFV may occur at enhanced rates in supersymmetric extensions of the standard model, giving rise to observable LFV signals [13,35–39].

We analyze this possibility within the constrained minimal supersymmetric standard model (CMSSM) with universal scalar, gaugino masses and trilinear terms at the GUT scale (m_0, $M_{1/2}$ and A_0, respectively), using mass matrices that are inspired by GUT models with Abelian flavor symmetries [40,41]. These textures reproduce naturally the observed fermion mass hierarchies and mixing angles and may also have interesting implications for leptogenesis [42–45]. Despite their phenomenological appeal, however, there are ambiguities and limitations due to the fact that the entries in the mass matrices are determined only up to $\mathcal{O}(1)$ numerical factors.

The paper is organized in the following way: In Sec. II we look at the theoretical and phenomenological predictions for neutrino mass matrices. In Sec. III A we discuss the origin of LFV in representative supersymmetric scenarios, in Sec. III B we analyze the connection between the U(1) charges and LFV and in Sec. III C we discuss the numerical procedure and the renormalization-group runs. The obtained mixing matrices are then used to study various LFV processes: in Sec. III D we discuss radiative decays and the impact of the new $\mu \to e\gamma$ MEG bound on the parameter space of interest; in Sec. III E we study LFV in χ_2 decays at the LHC, while LFV from slepton production and decay at a future LC is discussed in Sec. III F. In Sec. IV we discuss possible implications for leptogenesis, and finally in Sec. V we summarize the main results of the paper.

II. NEUTRINO MASS TEXTURES INSPIRED BY SU(5)

Over the recent years, a plethora of textures have been proposed to explain the data on neutrino masses and mixing. The new data on θ_{13} provide additional constraints, excluding certain possibilities and constraining others. Rather than reviewing the vast literature on the subject, we choose a representative model that fits the fermion data and is well motivated on theoretical grounds. Nevertheless, we try to keep the results as generic as possible, placing emphasis on the links between physical observables. We also keep in mind that several *a priori* different theoretical models may converge to similar phenomenology, since they are matched to the same data.

The example we choose is provided by a SU(5) GUT combined with family symmetries [40,41]. The mass matrices are constructed by looking at the field content of the SU(5) representations, namely: three families of $(Q, u^c, e^c)_i \in \mathtt{10}$ representations, three families of $(L, d^c)_i \in \bar{\mathtt{5}}$ representations, and heavy right-handed neutrinos in singlet representations. This model therefore has the following properties: (i) the up-quark mass matrix is symmetric, and (ii) the charged lepton mass matrix is the transpose of the down-quark mass matrix, which relates the mixing of the left-handed leptons to that of the right-handed down-type quarks. Since the observed Cabibbo-Kobayashi-Maskawa mixing in the quark sector is due to a mismatch between the mixing of the left-handed up- and down-type quarks, it can be easily reconciled with a large atmospheric neutrino mixing.

Within this framework, and following for example [40,41,46], the Yukawa matrices have the form

$$Y_u \propto \begin{pmatrix} \varepsilon^6 & \varepsilon^5 & \varepsilon^3 \\ \varepsilon^5 & \varepsilon^4 & \varepsilon^2 \\ \varepsilon^3 & \varepsilon^2 & 1 \end{pmatrix}, \qquad Y_\ell \propto Y_d^T \propto \begin{pmatrix} \varepsilon^4 & \varepsilon^3 & \varepsilon \\ \varepsilon^3 & \varepsilon^2 & 1 \\ \varepsilon^3 & \varepsilon^2 & 1 \end{pmatrix},$$
$$Y_\nu \propto \begin{pmatrix} \varepsilon^{|1\pm n_1|} & \varepsilon^{|1\pm n_2|} & \varepsilon^{|1\pm n_3|} \\ \varepsilon^{|n_1|} & \varepsilon^{|n_2|} & \varepsilon^{|n_3|} \\ \varepsilon^{|n_1|} & \varepsilon^{|n_2|} & \varepsilon^{|n_3|} \end{pmatrix}, \tag{4}$$

where $Y_{u,d,\ell,\nu}$ stand for the Yukawa couplings of quarks, charged leptons and neutrinos, respectively, and n_i denote the U(1) charges of the heavy Majorana neutrinos. The heavy Majorana mass matrix is then given by

$$M_N \propto \begin{pmatrix} \varepsilon^{2|n_1|} & \varepsilon^{|n_1+n_2|} & \varepsilon^{|n_1+n_3|} \\ \varepsilon^{|n_1+n_2|} & \varepsilon^{2|n_2|} & \varepsilon^{|n_2+n_3|} \\ \varepsilon^{|n_1+n_3|} & \varepsilon^{|n_2+n_3|} & \varepsilon^{2|n_3|} \end{pmatrix}. \tag{5}$$

There is no unique choice for the right-handed neutrino charges n_1, n_2, n_3, and several possibilities may be compatible with the low-energy neutrino data. We know, however, that the neutrino masses and mixing angles are related to the $\nu_L \nu_L$ contributions in the effective neutrino mass matrix

$$m_{\text{eff}} \approx m_\nu^D \frac{1}{M_N} m_\nu^{DT}, \tag{6}$$

which, if calculated from the matrices in (4) and (5), is of the form

$$m_{\text{eff}} \propto \begin{pmatrix} \varepsilon^2 & \varepsilon & \varepsilon \\ \varepsilon & 1 & 1 \\ \varepsilon & 1 & 1 \end{pmatrix}. \tag{7}$$

This form of m_{eff} is quite natural in the simplest seesaw models with a single expansion parameter and generic structures for the heavy and light Majorana mass matrices, due to cancellations that eliminate the dependences on the right-handed charges. Its predictions have been extensively analyzed from a phenomenological point of view [47–56] and give a reasonable match to the data, provided there are no cancellations of potentially large mixings in the charged lepton sector. Among other predictions, θ_{13} turns out to be of the correct order of magnitude. It is interesting to also note that, to lowest order in ϵ, $Y_\ell Y_\ell^\dagger$ has the same structure as m_{eff}, namely

$$Y_\ell Y_\ell^\dagger \propto m_{\rm eff} \propto \begin{pmatrix} \varepsilon^2 & \varepsilon & \varepsilon \\ \varepsilon & 1 & 1 \\ \varepsilon & 1 & 1 \end{pmatrix}. \quad (8)$$

The flavor mixing matrices are determined by the following diagonalizations of the Dirac and Majorana mass matrices:

$$V_\ell^T (Y_\ell Y_\ell^\dagger) V_\ell^* = \mathrm{diag}(y_e^2, y_\mu^2, y_\tau^2), \quad (9)$$

$$V_D{}^T (Y_\nu Y_\nu{}^\dagger) V_D^* = \mathrm{diag}(y_{\nu_1}^2, y_{\nu_1}^2, y_{\nu_3}^2), \quad (10)$$

$$U_N{}^T M_N U_N = \mathrm{diag}(M_1, M_2, M_3), \quad (11)$$

$$U_\nu{}^T m_{\rm eff} U_\nu = \mathrm{diag}(m_{\nu_1}, m_{\nu_2}, m_{\nu_3}). \quad (12)$$

In terms of the above matrices, the Maki-Nakagawa-Sakata (MNS) matrix is given by

$$U_{\rm MNS} \equiv U = V_\ell^\dagger U_\nu \quad (13)$$

and can be parametrized as

$$U = V \cdot \mathrm{diag}(e^{-i\phi_1/2}, e^{-i\phi_2/2}, 1), \quad (14)$$

where

$$V = \begin{pmatrix} c_{12}c_{13} & s_{12}c_{13} & s_{13}e^{-i\delta} \\ -c_{23}s_{12} - s_{23}s_{13}c_{12}e^{i\delta} & c_{23}c_{12} - s_{23}s_{13}s_{12}e^{i\delta} & s_{23}c_{13} \\ s_{23}s_{12} - c_{23}s_{13}c_{12}e^{i\delta} & -s_{23}c_{12} - c_{23}s_{13}s_{12}e^{i\delta} & c_{23}c_{13} \end{pmatrix} \quad (15)$$

and c_{ij} and s_{ij} stand for $\cos\theta_{ij}$ and $\sin\theta_{ij}$, respectively.

A. Predictions for neutrino observables

Within the above framework there are ambiguities in the choices of coefficients, limited to a certain extent by requiring consistency with the experimental data. The match of the neutrino data to textures predicted by Abelian flavor symmetries can be made by treating coefficients as random variables in Monte Carlo scans of the multidimensional parameter space, in a statistical study of the probability that the textures can naturally reproduce the measured angles and masses [49–55].

Here, being interested in matrices that are naturally consistent with the neutrino data, we proceed by taking the expansion parameter to be $\varepsilon = 0.2$ and multiply the entries of Y_ℓ, Y_ν and M_N in Eqs. (4) and (5) by coefficients ℓ_{ij}, ν_{ij} and N_{ij} in the range $\pm[0.5, 2]$. In addition, we impose the following constraints:

(i) We select the charged lepton Yukawa coupling matrix Y_ℓ so that the correct charged lepton mass hierarchies are reproduced, namely

$$\frac{m_\mu}{m_\tau} \sim 0.06, \qquad \frac{m_e}{m_\tau} \sim 2.5 \times 10^{-3}. \quad (16)$$

(ii) Y_ν and M_N are required to give a light neutrino mass matrix $m_{\rm eff}$ of the form (7), with entries that deviate by a factor $\in [0.5, 2]$ from those in Eq. (7).

(iii) We impose normal hierarchy among the neutrino masses. We fix $m_{\nu_3} \sim \sqrt{\Delta m^2_{\rm atm}} \sim 0.05$ eV and require $0.16 < m_{\nu_2}/m_{\nu_3} < 0.19$, $m_{\nu_1} < 0.2 m_{\nu_2}$ consistent with the measured values of $\Delta m^2_{\rm sol}$ and $\Delta m^2_{\rm atm}$ [57].

(iv) We require the following range of mixing angles [7]:

$$0.27 < \sin^2\theta_{12} < 0.35,$$
$$0.34 < \sin^2\theta_{23} < 0.67, \quad (17)$$
$$0.018 < \sin^2\theta_{13} < 0.033.$$

The range on θ_{13} is consistent with the values reported by both [10,11] at the 3σ level.

(v) We make a further selection by requiring that the hierarchy of eigenvalues of $Y_\ell Y_\ell^\dagger$ (which, as discussed above, has a similar structure to $m_{\rm eff}$ and $Y_\nu Y_\nu^\dagger$) preserves the order of the gauge eigenstates. This reduces the density of solutions in the plots and implies large off-diagonal elements in both V_ℓ and U_ν.

The selection of coefficients in the textures is performed so that the above conditions are satisfied and the coefficients are chosen to be real in the range $\pm[0.5, 2]$. Given our ignorance of the CP-violating phase δ, we focus on the case $\delta = 0$ and do not include the Majorana phases $\phi_{1,2}$.

In Table I we provide two representative examples of our fits, which will be used for our analysis below. We quote our predictions for neutrino mixing angles with and without taking into account renormalization effects. The RGE runs for the "seesaw" MSSM are evaluated using the code REAP, described in Ref. [58]. The coefficients are taken at the GUT scale. We work with $\tan\beta = 45$, since this is the largest value that we will use in the numerical computations of the next section (and larger $\tan\beta = 45$ results to larger corrections). In all cases, the effect of varying $\tan\beta$ in the range of values used in our examples (from 16 to 45) has an impact of less than 2% on the final value of the neutrino mixing angles.

In Fig. 1 we present the predictions for the neutrino mixing angles corresponding to the above criteria. Here

TABLE I. Indicative textures for Y_ℓ, Y_ν and M_N at the GUT scale, to be studied in detail below. The n_i are Abelian charges, that can only be constrained by LFV. The computation of the neutrino mixing angles includes the renormalization-group equation (RGE) effects using $\tan\beta = 45$ (in parentheses we quote the predictions without the RGE runs).

Fit	Y_ℓ	Y_ν	M_N
1	$\begin{pmatrix} \varepsilon^4 & -1.6\varepsilon^3 & 1.2\varepsilon \\ 0.7\varepsilon^3 & 1.6\varepsilon^2 & -0.6 \\ 0.7\varepsilon^3 & -1.7\varepsilon^2 & -1.3 \end{pmatrix}$	$\begin{pmatrix} \varepsilon^{\lvert 1\pm n_1\rvert} & \varepsilon^{\lvert 1\pm n_2\rvert} & -1\varepsilon^{\lvert 1\pm n_3\rvert} \\ 0.8\varepsilon^{\lvert n_1\rvert} & \varepsilon^{\lvert n_2\rvert} & -1.2\varepsilon^{\lvert n_3\rvert} \\ -1.3\varepsilon^{\lvert n_1\rvert} & \varepsilon^{\lvert n_2\rvert} & 0.7\varepsilon^{\lvert n_3\rvert} \end{pmatrix}$	$\begin{pmatrix} \varepsilon^{2\lvert n_1\rvert} & \varepsilon^{\lvert n_1+n_2\rvert} & -1.7\varepsilon^{\lvert n_1+n_3\rvert} \\ \varepsilon^{\lvert n_1+n_2\rvert} & \varepsilon^{2\lvert n_2\rvert} & \varepsilon^{\lvert n_2+n_3\rvert} \\ -1.7\varepsilon^{\lvert n_1+n_3\rvert} & \varepsilon^{\lvert n_2+n_3\rvert} & -\varepsilon^{2\lvert n_3\rvert} \end{pmatrix}$
	$\sin^2\theta_{13} = 0.020(0.022),$	$\sin^2\theta_{12} = 0.267(0.274)$	$\sin^2\theta_{23} = 0.580(0.613)$
2	$\begin{pmatrix} \varepsilon^4 & -1.5\varepsilon^3 & -2\varepsilon \\ \varepsilon^3 & -1.9\varepsilon^2 & 0.5 \\ 0.5\varepsilon^3 & -\varepsilon^2 & 0.75 \end{pmatrix}$	$\begin{pmatrix} \varepsilon^{\lvert 1\pm n_1\rvert} & \varepsilon^{\lvert 1\pm n_2\rvert} & -2\varepsilon^{\lvert 1\pm n_3\rvert} \\ 1.5\varepsilon^{\lvert n_1\rvert} & \varepsilon^{\lvert n_2\rvert} & -0.75\varepsilon^{\lvert n_3\rvert} \\ 1.9\varepsilon^{\lvert n_1\rvert} & \varepsilon^{\lvert n_2\rvert} & 1.5\varepsilon^{\lvert n_3\rvert} \end{pmatrix}$	$\begin{pmatrix} \varepsilon^{2\lvert n_1\rvert} & \varepsilon^{\lvert n_1+n_2\rvert} & -1.9\varepsilon^{\lvert n_1+n_3\rvert} \\ \varepsilon^{\lvert n_1+n_2\rvert} & \varepsilon^{2\lvert n_2\rvert} & \varepsilon^{\lvert n_2+n_3\rvert} \\ -1.9\varepsilon^{\lvert n_1+n_3\rvert} & \varepsilon^{\lvert n_2+n_3\rvert} & 1.9\varepsilon^{2\lvert n_3\rvert} \end{pmatrix}$
	$\sin^2\theta_{13} = 0.017(0.022)$	$\sin^2\theta_{12} = 0.278(0.310)$	$\sin^2\theta_{23} = 0.390(0.439)$

we do not take into account the RGE run of the mass matrices, since these effects will not affect the global picture of the solutions displayed in Fig. 1. Within this class of models, most of the solutions that reproduce the correct range of θ_{12} and θ_{23} also predict a neutrino mixing angle θ_{13} that is compatible with the data from [10,11]. Within the range of θ_{13} the model predictions are mostly in the mid-lower range of θ_{12}. On the other hand, in the case of θ_{23}, a higher density of solutions is found in the mid-higher range of θ_{23}. We note that the number of fits predicting the maximal value $\theta_{23} = \pi/4$ is smaller when we impose the hierarchy condition (iii), as compared to the case where only the experimental bounds on $\Delta^2 m_{\rm sol}$ and $\Delta^2 m_{\rm atm}$ are considered. This is consistent with the observed deviation of θ_{23} from its maximal value [57].

As benchmarks for studying LFV in subsequent sections, we have identified the two sets of textures of Table I and indicated with crosses in Fig. 1. These benchmarks are chosen as representatives of the two different regions identified in the global statistical data analysis performed in [57] and also shown in Fig. 1. Fit 1 lies in the right region of the right panel of Fig. 1, with larger θ_{23}, and fit 2 lies in the left region of the same panel, with smaller θ_{23}.

We would like to point out that the fits in Fig. 1 are independent of the charges n_i, which affect Y_ν and M_N but not their combination in $m_{\rm eff}$. On the other hand, the choices of n_i do affect the rates for charged LFV processes,

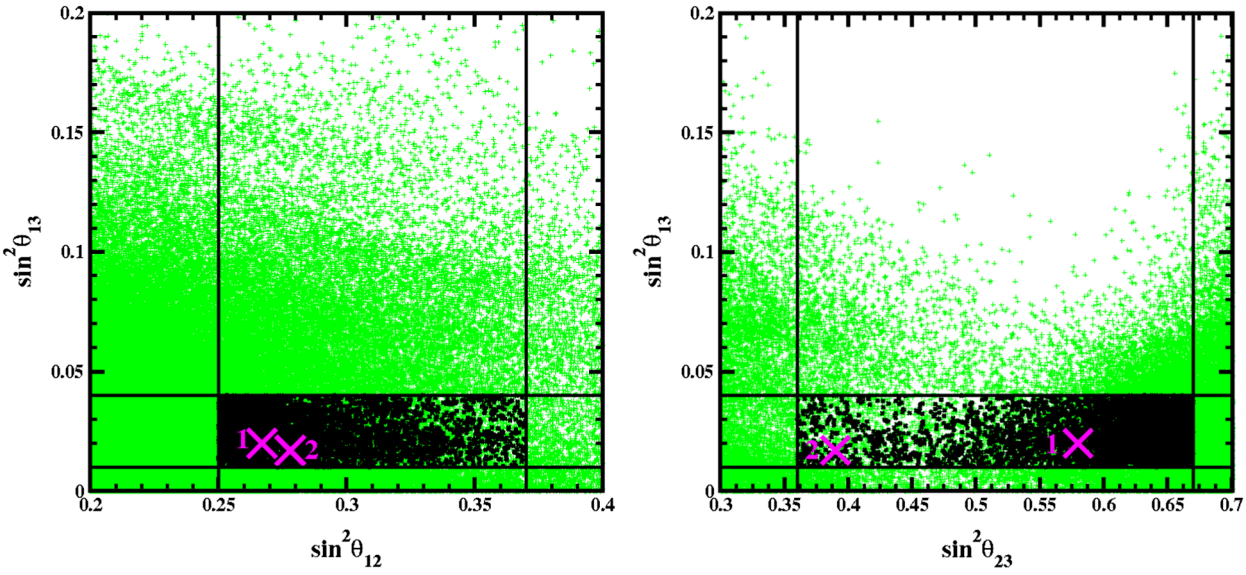

FIG. 1 (color online). We summarize the correlations between the neutrino mixing angles before and after constraining the model coefficients (as discussed in the text). The solid lines indicate the experimental bounds, and the small black crosses represent models satisfying all constraints. The two large crosses correspond to the benchmark models that are discussed in the text and in Table I and are used for numerical calculations.

as we will show in the next section. Charged LFV processes are therefore powerful probes of parameters that cannot be constrained by lepton hierarchies and better measurements of the neutrino parameters.

III. CHARGED LEPTON FLAVOR VIOLATION

A. Slepton masses in seesaw models

The neutrino mass textures discussed above arise naturally from SU(5) enhanced by a U(1) flavor symmetry. In order to study LFV processes, however, we are guided to a large extent by phenomenological considerations and thus our results are more generic. The benchmark solutions previously identified, which naturally reproduce the correct neutrino phenomenology, are used to obtain the matrices that determine the LFV vertices in the context of the CMSSM (extended with right-handed heavy Majorana neutrinos arising from a seesaw mechanism).

Since the Dirac neutrino and charged lepton Yukawa couplings cannot, in general, be diagonalized simultaneously (and since both types of lepton Yukawa couplings appear in the RGEs), the lepton Yukawa matrices and the slepton mass matrices at low energies cannot be diagonalized simultaneously, either. In the basis where the charged lepton masses m_ℓ are diagonal, the soft slepton-mass matrix acquires corrections that contain off-diagonal contributions from renormalization at scales below $M_{\rm GUT}$, of the following form in the leading-log approximation [35]:

$$\delta m_{\tilde{\ell}}^2 \propto \frac{1}{16\pi^2}(6m_0^2 + 2A_0^2) Y_\nu{}^\dagger Y_\nu \ln\left(\frac{M_{\rm GUT}}{M_N}\right). \quad (18)$$

Here M_N is the intermediate scale where the effective neutrino-mass operator is formed. The physical charged slepton masses are obtained by numerical diagonalization of the following 6×6 matrix:

$$m_{\tilde{\ell}}^2 = \begin{pmatrix} m_{LL}^2 & m_{LR}^2 \\ m_{RL}^2 & m_{RR}^2 \end{pmatrix}, \quad (19)$$

where all the entries are 3×3 matrices in flavor space. Using the basis where Y_ℓ is diagonal, it is convenient to write the 3×3 entries of (19) in the form

$$m_{LL}^2 = (m_{\tilde{\ell}}^{\rm diag})^2 + \delta m_{\tilde{\ell}}^2 + m_\ell^2 - \frac{1}{2}(2M_W^2 - M_Z^2)\cos 2\beta, \quad (20)$$

$$m_{RR}^2 = (m_{\tilde{\ell}_R}^{\rm diag})^2 + m_\ell^2 - (M_Z^2 - M_W^2)\cos 2\beta, \quad (21)$$

$$m_{RL}^2 = (A_\ell^{\rm diag} + \delta A_\ell - \mu\tan\beta) m_\ell, \quad (22)$$

$$m_{LR}^2 = m_{RL}^{2\dagger}. \quad (23)$$

Here $\tan\beta$ is the ratio of the two MSSM Higgs vacuum expectation values (VEVs), $(m_{\tilde{\ell}}^{\rm diag})^2$, $(m_{\tilde{\ell}_R}^{\rm diag})^2$ and $A_\ell^{\rm diag}$ denote the diagonal contributions to the corresponding matrices, obtained by numerical integration of the RGEs, and $\delta m_{\tilde{\ell}}^2$ and δA_ℓ denote the corrections to off-diagonal terms that appear because Y_ν and Y_ℓ cannot be diagonalized simultaneously.

The full mass matrix for left- and right-handed sneutrinos has a 12×12 structure, given in terms of 3×3 Dirac, Majorana and sneutrino mass matrices. The effective 3×3 mass-squared matrix for the left-handed sneutrinos has the same form as the m_{LL}^2 part (23) of the 6×6 charged slepton matrix (19), with the difference that now the Dirac masses are absent. In Ref. [36] it was shown that is sufficient to use

$$m_{\tilde{\nu}}^2 = (m_{\tilde{\ell}}^{\rm diag})^2 + \delta m_{\tilde{\ell}}^2 + \frac{1}{2}M_Z^2\cos 2\beta. \quad (24)$$

The matrix responsible for LFV in the lepton-slepton-gaugino vertices is

$$V_{\rm LFV} = V_D^\dagger V_\ell, \quad (25)$$

and the slepton mass matrices contain off-diagonal terms generated by

$$m_{LL}^2 = V_{\rm LFV}^\dagger (m_{LL}^2)_{\rm d} V_{\rm LFV}, \quad (26)$$

while the A terms become

$$A_\ell = V_{\rm LFV}^T (A_\ell)_{\rm d}. \quad (27)$$

Here $(m_{LL}^2)_{\rm d}$ and $(A_\ell)_{\rm d}$ are the terms resulting from the RGE running of the universal soft terms at the GUT scale in a basis where Y_ν is diagonal. The corresponding effects in $m_{\tilde{R}R}^2$ are negligible and are not considered in the numerical calculations.

We remark that, in general, in the framework of supersymmetric (SUSY) SU(5) GUT with U(1) family symmetries, flavor dynamics are linked to scalar singlet fields, flavons, whose nonzero vacuum expectation value breaks the U(1) symmetry. The RGE running of the parameters above the GUT scale due to flavons dynamic induces flavor-dependent corrections to sfermion soft mass matrices and A terms and thus potentially large LFV effects [36,59–62]. However, while flavon effects can be potentially very large, we know from flavor phenomenology that this is not the case and that they have to be suppressed to the point that they are comparable to the effects we consider here. Such a suppression can be achieved, among others, in an scenario where the effect of nonuniversal soft terms is diminished by RGE effects beyond the GUT scale, as indicated in [46]. Given that the exact knowledge of flavon effects depends on model building and physics of unknown scales (supersymmetry breaking scale, flavon dynamics scale or string scale), a complete mechanism canceling the undesired

TABLE II. Values for the matrix $V_{\rm LFV}$ of Eq. (25) corresponding to fit 2 of Table I with $\varepsilon = 0.2$ and different choices of the U(1) charges, Eqs. (4) and (5).

	(i)	(ii)	(iii)	(iv)
n_i	$\{n_1 = 1, n_2 = 0, n_3 = 0\}$	$\{n_1 = 2, n_2 = 1, n_3 = 0\}$	$\{n_1 = 2, n_2 = 0, n_3 = 1\}$	$\{n_1 = 0, n_2 = 1, n_3 = 0\}$
$V_{\rm LFV}$	$\begin{pmatrix} 0.805 & -0.385 & -0.451 \\ 0.182 & 0.885 & -0.429 \\ 0.565 & 0.263 & 0.782 \end{pmatrix}$	$\begin{pmatrix} 0.805 & -0.385 & -0.452 \\ -0.064 & 0.700 & -0.711 \\ 0.590 & 0.601 & 0.539 \end{pmatrix}$	$\begin{pmatrix} -0.805 & 0.384 & 0.453 \\ 0.544 & 0.782 & 0.305 \\ -0.237 & 0.492 & -0.838 \end{pmatrix}$	$\begin{pmatrix} 0.806 & -0.401 & -0.436 \\ -0.437 & -0.899 & 0.016 \\ -0.399 & 0.178 & -0.901 \end{pmatrix}$

flavor-violating soft terms at $M_{\rm GUT}$ goes beyond the scope of this paper.

B. LFV and neutrinos

We now study the conditions under which the favored range of neutrino masses and mixing can lead in a natural way to observable signatures for charged LFV. As already discussed, while the neutrino parameters are independent of the charges n_i, this is not the case for LFV. As a result, LFV can provide a way to probe the right-handed neutrino sector, for which only limited information is available.

In Sec. II A, we identified two representative benchmark fits suitable for studying charged LFV. The level of charged LFV is determined by the product $V_{\rm LFV} = V_D^\dagger V_\ell$, and thus by the charges n_i which enter in the Dirac neutrino mixing matrix $V_D^\dagger$. Having a V_ℓ with large off-diagonal 1–2 and 2–3 entries is a natural choice to match the lepton data. Then, different choices of n_i lead to different possibilities for $V_D^\dagger$; in fact, there are two possibilities associated with a V_ℓ with large off-diagonal elements: (i) The charge combinations generate a $V_D^\dagger$ with small off-diagonal elements; in this case, $V_{\rm LFV} \sim V_\ell$. (ii) The off-diagonal elements of $V_D^\dagger$ are large, but multiplied with V_ℓ, they can give either large or small elements in $V_{\rm LFV}$ depending on coefficients and phases.

An illustration of the dependences of the entries in $V_{\rm LFV}$ on the different right-handed neutrino charges is given in Table II. For simplicity, we focus on fit 2, noting that similar results hold for fit 1. The matrix (i) is an example of case (i), with small off-diagonal elements in V_D. In (ii) and (iii), V_D has large off-diagonal elements which enhance $V_{\rm LFV}$. Finally in (iv), V_D has large off-diagonal elements but cancellations with V_ℓ occur in the 2–3 sector, suppressing LFV.

C. Numerical procedure and RGEs

The recent LHC measurement of the Higgs mass [63,64] imposes severe constraints in the CMSSM parameter space. More specifically, a Higgs mass of $m_h \sim 125$ GeV implies, in general, a relatively heavy sparticle spectrum, which is consistent with the cosmological constraint on the neutralino relic density only in limited regions. A global analysis of the CMSSM parameter space was performed in [65], yielding two almost equally good fits to the available data, one with relatively low sparticle masses and $\tan\beta \sim 16$, and the other with larger sparticle masses and $\tan\beta \sim 45$[1]:

$$\begin{aligned} &\text{(a)}\ \tan\beta = 16, \quad m_0 = 300\ \text{GeV}, \\ &\quad M_{1/2} = 910\ \text{GeV}, \quad A_0 = 1320\ \text{GeV}, \\ &\text{(b)}\ \tan\beta = 45, \quad m_0 = 1070\ \text{GeV}, \\ &\quad M_{1/2} = 1890\ \text{GeV}, \quad A_0 = 1020\ \text{GeV}. \end{aligned} \tag{28}$$

The sign of μ is positive, as favored by $g_\mu - 2$ measurements. Regarding cosmological considerations, point (a) belongs to the area where the WMAP-favored range of $\Omega_\chi h^2$ is obtained via $\chi - \tilde\tau$ coannihilation,[2] whereas point (b) lies in the funnel region where the neutralino LSP annihilates rapidly via direct-channel H/A poles.

We evaluate the RGEs using universal soft terms at the GUT scale, $M_{\rm GUT}$. The standard model parameters are evaluated at M_Z and $m_t(m_t)$. At the GUT scale, defined as the meeting point of the gauge couplings g_1 and g_2 [g_3 is set so that $\alpha_s(m_Z) = 0.1172$], we work in a basis where Y_ν is diagonal. Nondiagonal elements of the soft mass matrices are induced from the fact that Y_ℓ cannot be diagonalized simultaneously with Y_ν. The right-handed neutrino scale is identified with the mass of the largest eigenvalue of M_N, M_3. The coupling Y_{ν_3} is calculated by requiring that $m_{\nu_3} = 0.05$ eV at low energy, using the respective RGE [38,68,69]. At M_3 we decouple the seesaw parameters from the RGE; in doing so, we neglect the effect of the lighter neutrinos, which in the case of hierarchical neutrinos is not large (even if M_2 and M_3 are much lighter than M_3, the corresponding Y_ν must decrease according to the seesaw relation, resulting to an insignificant impact on the slepton mass running). At M_3 we rotate all the fields in the basis where Y_ℓ becomes diagonal; in this basis, m^2_{LL}

[1]Note that our A_0 values have opposite sign with respect to those of Ref. [65] where the authors use a definition for the trilinear scalar coupling that differs from the one in standard codes like SUSPECT and SOFTSUSY.

[2]We note that in this region the $\chi - \tilde\tau$ mass difference is very small, offering other experimental challenges and opportunities [66,67].

and A_ℓ take the form of Eqs. (26) and (27) while $m^2_{\tilde{R}R}$ remains essentially diagonal since its RGE is not affected by Y_ν. Moreover, in this basis, only the diagonal terms evolve from M_3 down to low energies. The matrix $V_{\rm LFV}$ is computed using Yukawa textures that match the neutrino data. In our RGE analysis we do take into account the change of the overall scale of $m_{\rm eff}$ and Y_ℓ but not the RGE dependence of each matrix element (for hierarchical neutrinos this dependence is small and can be absorbed in the uncertainty of the coefficients used to fit the texture without a significant effect in the slepton mass matrices). At low energies, we decouple the SUSY particles at $M_{\rm SUSY} = \sqrt{m_{\tilde{l}_1} \cdot m_{\tilde{l}_2}}$ and continue with the SM RGEs to m_t and M_Z, with the initial conditions of the RGEs being iteratively adjusted to the experimental data.

D. Predictions for radiative decays

The matrix element of the electromagnetic-current operator between two distinct lepton mass eigenstates ℓ_i and ℓ_j is given in general by

$$\begin{aligned}\mathcal{T}_\lambda &= \langle \ell_i|(p-q)|\mathcal{J}_\lambda|\ell_j(p)\rangle \\ &= \bar{u}_i(p-q)[m_j i\sigma_{\lambda\beta}q^\beta(A^L_M P_L + A^R_M P_R) \\ &\quad + (q^2\gamma_\lambda - q_\lambda \gamma\cdot q)(A^L_E P_L + A^R_E P_R)]u_j(p), \end{aligned} \tag{29}$$

where q is the photon momentum. The coefficients A_M and A_E denote contributions from neutralino/charged slepton and chargino/sneutrino exchanges. The amplitude of the LFV process is then proportional to $\mathcal{T}_\lambda \epsilon^\lambda$, where ϵ^λ is the photon-polarization vector. The branching ratios (BR) of

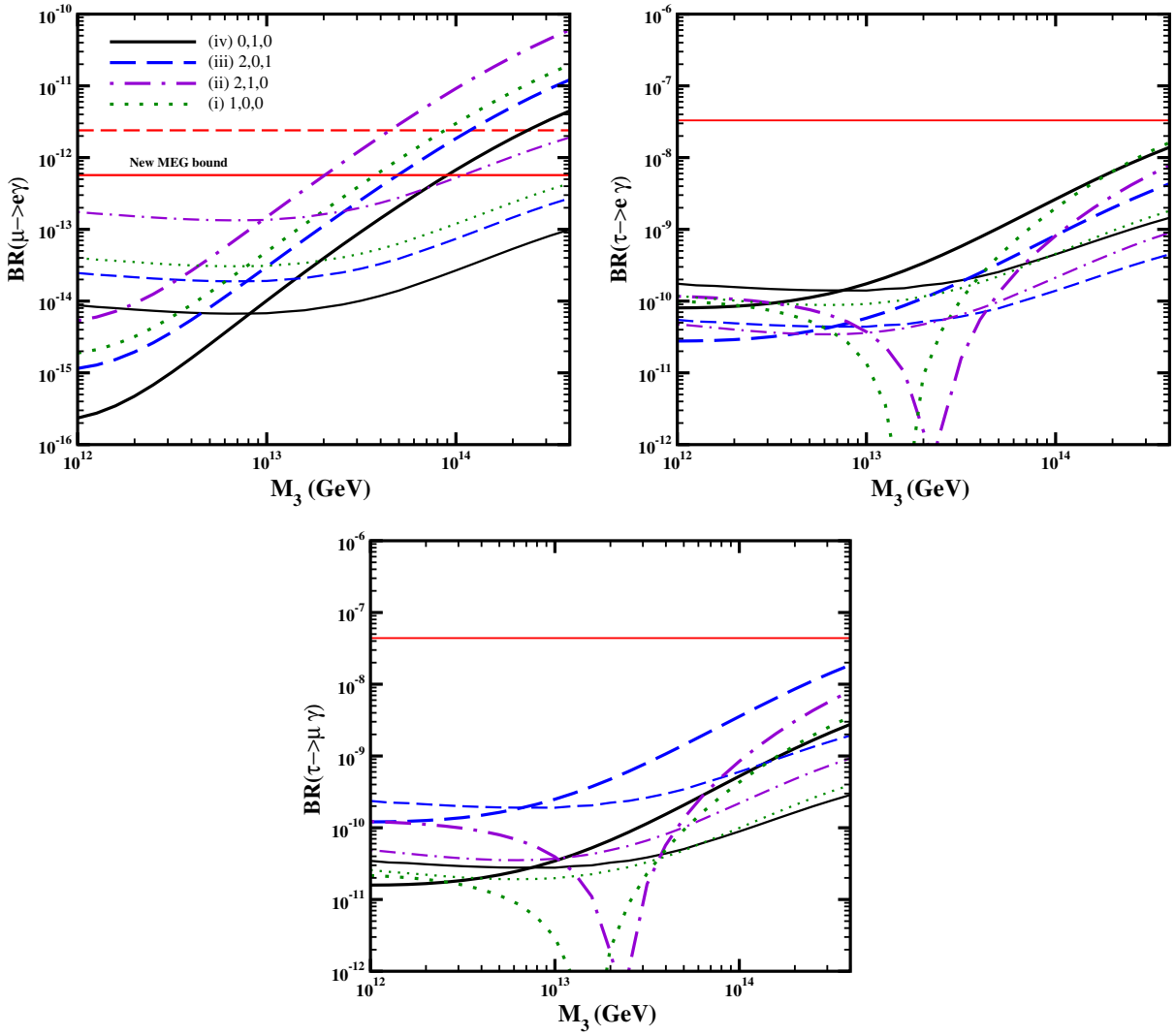

FIG. 2 (color online). Predictions for the rare LFV decays $\ell_i \to \ell_j\gamma$ as a function of the right-handed neutrino mass M_N, for the benchmark points displayed in (28) (a) (thick line) and (b) (thin line), using the neutrino mixing fits shown in Table III. The solid lines correspond to case (iv), dashed ones to (iii), dot-dashed to (ii) and dotted to (i). The horizontal solid lines indicate the current experimental upper bounds, while the dashed lines correspond to the previous MEG limit on BR($\mu \to e\gamma$).

the decays $\ell_j \to \ell_i + \gamma$ are calculated using the exact formulas of Ref. [35].

In Fig. 2 we show numerical predictions for the LFV branching ratios arising from the textures introduced above and for the CMSSM parameters specified in (28). We show the effect of varying M_3 from 6×10^{14} GeV down to 10^{12} GeV, for fit 2 of Table I and for the choices of right-handed neutrino charges of Table II. We can see that the experimental upper bounds on $\mathrm{BR}(\mu \to e\gamma)$ can be reached with some of the Yukawa textures we studied, even with the heavy sparticle spectrum implied by the benchmark point (a). The new MEG bound on $\mathrm{BR}(\mu \to e\gamma)$ imposes constraints on the seesaw scale for all charge choices of Table II for point (a), and for fit (ii) at point (b).

In the case of point (a), we find cancellations that reduce the branching ratios for some neutrino mixing fits. This happens because of the large value of A_0, which leads to significant cancellations among the different LFV decay amplitudes [35–37]. For the fits (i) and (ii) we find this type of cancellation in $\mathrm{BR}(\tau \to \mu\gamma)$ and $\mathrm{BR}(\tau \to e\gamma)$, for a range of values of the right-handed neutrino scale M_3. This is due to the fact that, at large values of A_0, the contribution A_M^R from the neutralino/charged slepton loops in Eq. (29) cancels with the one arising from chargino/sneutrino loops, A_E^R, which is the dominant contribution for small A_0. The ratio of these two contributions can be modulated by the parameters that determine the size of the flavor mixing elements $\delta m_{\tilde{\ell}}^2$ in Eq. (23). In our case the scale of M_3 also determines the strength of Y_ν and thus the size of the LFV terms. We use Fig. 2 and the current MEG bound on $\mathrm{BR}(\mu \to e\gamma)$ to fix the M_3 scale for further studies: $M_3 = 2 \times 10^{13}$ GeV for the benchmark point (a) and $M_3 = 10^{14}$ GeV for the benchmark point (b).

E. LFV in χ_2 decays at the LHC

A promising channel to search for LFV at the LHC is the production and decay of the second lightest neutralino, $\chi_2 \to \chi + \tau^\pm \mu^\mp$. In [26,29] it was shown that in order to have a signal that could be distinguished from the background, the ratio

$$R_{\tau\mu} = \Gamma(\chi_2 \to \chi + \tau^\pm + \mu^\mp)/\Gamma(\chi_2 \to \chi + \tau^\pm + \tau^\mp) \quad (30)$$

should be of the order of 10%. For $A_0 = 0$, due to the absence of cancellations suppressing rare charged lepton decays, one had to go beyond the CMSSM to find solutions compatible with all experimental and cosmological data [29]. Here, we extend this study to large values of A_0, noting that the cancellations that can arise in the branching ratios of radiative decays do not occur in $R_{\tau\mu}$. This opens the possibility to observe LFV in neutralino decays at the LHC, in cases where LFV would be undetectable in rare charged lepton radiative decays.

To see whether this is indeed the case, we proceed with the computation including all contributing on-shell sfermion exchange diagrams, as given in [28]:

$$\begin{aligned}\mathrm{BR}(\chi_2 \to \chi\tau^\pm\mu^\mp) &= \sum_{i=1}^{3}[\mathrm{BR}(\chi_2 \to \tilde{\ell}_i\mu)\mathrm{BR}(\tilde{\ell}_i \to \tau\chi) \\ &\quad + \mathrm{BR}(\chi_2 \to \tilde{\ell}_i\tau)\mathrm{BR}(\tilde{\ell}_i \to \mu\chi)]. \end{aligned} \quad (31)$$

These are evaluated in the benchmark points (a) and (b), to see whether the branching ratio can be of the order of the required reference value.

In Fig. 3 we present the predictions for the branching ratio (30) as a function of M_3. For point (a), our predictions are within the reach of the LHC for values of M_3 that are compatible with the MEG limit. For point (b), the predictions are below the expected experimental sensitivity.

F. LFV at a linear collider

In supersymmetric models where LFV is produced by lepton-slepton vertices, observable signatures may occur either directly, in slepton-pair production, or indirectly, via slepton production in cascade decays [17]. If the flavor mixing is introduced in the left-left slepton sector, as is the case for the models under consideration here, the dominant channels are slepton-pair production and LFV decays, such as

$$\begin{aligned} e^+e^- &\to \tilde{\ell}_i^-\tilde{\ell}_j^+ \to \tau^\pm\mu^\mp\tilde{\chi}_1^0\tilde{\chi}_1^0, \\ e^+e^- &\to \tilde{\nu}_i\tilde{\nu}_j^c \to \tau^\pm\mu^\mp\tilde{\chi}_1^+\tilde{\chi}_1^-. \end{aligned} \quad (32)$$

In the CMSSM benchmark points introduced above, the channel mediated by charged sleptons clearly dominates over the sneutrino-pair production process and may lead to a cross section of the order of 1 fb; this is the reference value of [23], for a LFV signal of $\mu^\pm\tau^\pm$ pairs that can be distinguished from the background, according to the study made in [21]. Here, we extend our previous results [23] which were focused on the production of $\mu^\pm\tau^\pm$ pairs by considering the full structure of the Yukawa matrices, thus comparing the LFV production of charged leptons of all generations. Complete expressions for the LFV cross sections are given in Ref. [18] and used in our work.

In Fig. 4 we present the expected cross sections $\sigma(e^+e^- \to \tilde{\ell}_i^-\tilde{\ell}_j^+ \to \ell_a^\pm\ell_b^\mp + 2\chi^0)$ as a function of $\sqrt{s}$ for the same choice of parameters as in Figs. 2 and 3. Naturally, the cross sections in the case of point (a) are larger because sleptons and gauginos are much lighter than in the spectrum of point (b). In (a) sleptons and sneutrinos are nearly degenerate and the cross sections, at energies above the threshold for pair production that is around 1.2 TeV, show a feeble decrease with $\sqrt{s}$. Final states with $e\mu$ pairs have the largest cross section, with value between 1 and 10 fb, with a small dependence on the choice of charges (i)–(iv). On the other hand, the cross section for the processes with τe and $\tau\mu$ final states shows a stronger dependence on the choice of charges, varying between 10^{-1} and 1 fb in the first case, and between 10^{-2} and 1 fb in the second case. Similar behavior is observed in

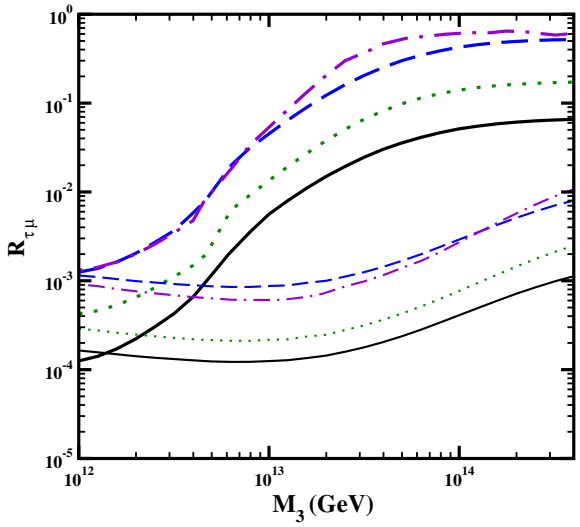

FIG. 3 (color online). The ratio defined in Eq. (30) is presented for the CMSSM points (a) (thick line) and (b) (thin line) [in Eq. (28)], with the same notation as in Fig. 2.

the case of point (b) where the heavy spectrum implies a threshold around 3 TeV and cross sections below 10^{-1} fb.

According to Fig. 2, at the selected value of $M_3 = 2 \times 10^{13}$ GeV, BR($\tau \to \mu\gamma$) and BR($\tau \to e\gamma$) are suppressed. Since these cancellations do not occur for the LFV LC signals, it is possible to observe slepton flavor oscillations at the LC, in cases where LFV would be undetectable in rare charged lepton decays (as it could also happen at the LHC). It is worth to remark that the CLIC project for a linear collider has as nominal center-of-mass energies the values 1.4 and 3 TeV [70,71], with the option of reaching 5 TeV. The value $\sqrt{s} = 1.4$ TeV is optimal for point (a) where the LFV cross sections are nearly maximal.

IV. LFV AND LEPTOGENESIS

We comment now on possible links between our LFV predictions and leptogenesis [42] through the decays of heavy, right-handed Majorana neutrinos into leptons and antileptons. Since LFV is related to the seesaw parameters in our framework, there can be interesting consequences for LFV in charged lepton decays and elsewhere [43].

In previous sections, we have used real parameters to fit the Yukawa couplings, but small phases that would not alter our LFV considerations could induce significant contributions to the lepton and baryon asymmetries of the universe. In what follows, we explore what sizes of the phases in Y_ν can predict a value for the baryon asymmetry Y_B compatible with the observation [72]

$$Y_B = (6.16 \pm 0.16) \times 10^{-10}. \tag{33}$$

For hierarchical heavy neutrinos in a supersymmetric seesaw model, one has [44]

$$Y_B \simeq -10^{-2} \kappa \epsilon_1, \tag{34}$$

where ϵ_1 is the CP-violating asymmetry in the decay of the lightest Majorana neutrino and κ an efficiency factor parametrizing the level of washout of the generated asymmetry by inverse decay and scattering interactions. The latter depends on the mass of the decaying neutrino M_1 and the effective mass parameter

$$\tilde{m}_1 = \frac{v_u^2}{M_1} (\lambda_\nu^\dagger \lambda_\nu)_{11}, \tag{35}$$

where λ_ν is the Dirac neutrino Yukawa matrix in the basis where the Majorana masses are diagonal, and v_u is the VEV of the Higgs field that couples to up quarks and neutrinos.

The CP-violating decay asymmetry ϵ_1 arises from the interference between tree-level and one-loop amplitudes:

$$\epsilon_1 = \frac{1}{(8\pi \lambda_\nu^\dagger \lambda_\nu)_{11}} \sum_{i \neq 1} \mathrm{Im}[((\lambda_\nu^\dagger \lambda_\nu)_{1i})^2] f\left(\frac{M_1^2}{M_i^2}\right), \tag{36}$$

with $f(y) = \sqrt{y}[\frac{1}{1-y} + 1 - (1+y)\ln(\frac{1+y}{y})]$. The value of the CP asymmetry depends on the details of the model, but a model-independent upper bound exists, given by [45]

$$|\epsilon_1| \leq \frac{3}{8\pi} \frac{M_1}{v_u^2} (m_3 - m_1), \tag{37}$$

where the m_i are the masses of the light neutrinos.

In our work, the flavor and GUT symmetries enable us to correlate M_1 with the mass of the heaviest right-handed neutrino, M_3, which controls the LFV effects. The neutrino Yukawa couplings of all generations are also related. Then, using as a first approximation Eq. (37) and κ as derived in [44], we can infer how leptogenesis may be accommodated in our study. Our fits predict large $\tilde{m}_1$ that, according to [44], implies a strong washout regime in which κ ranges between $\sim 10^{-3}$ and $\sim 10^{-4}$.

Some typical results are presented in Table III, where we see that at a reference value of $M_3 = 5 \times 10^{13}$ GeV, $Y_B^{\max}$ [calculated using ϵ_1 from Eq. (37)] is considerably larger than the experimental value of Y_B for fit (i), implying that in this case the CP-violating phases have to be small enough for ϵ_1 to be well below its maximal value. On the other hand, $Y_B^{\max}$ is below Y_B for fit (iii) and of the same order of magnitude for fits (ii) and (iv). These differences between the fits are due to the different hierarchies between the heavy Majorana masses and the neutrino Yukawa couplings in $\tilde{m}_1$ (which are determined by the right-handed neutrino charges). Consequently, they indicate how leptogenesis can be used as an additional probe of the right-handed neutrino sector, for which very limited information is provided by the neutrino data alone.

Looking at the predictions for leptogenesis in more detail and using the complete expression for ϵ_1 in (36),

TABLE III. Baryon asymmetry predictions based on four representative fits. Here, $Y_B^{\max}$ is the value obtained using Eq. (37), and Y_B^* is the prediction for Y_B using Eq. (36) and inserting a phase of 0.1 rad in the (12) element of Y_ν. In each row the upper value corresponds to $M_3 = 5 \times 10^{13}$ GeV and the lower to $M_3 = 10^{12}$ GeV.

	(i)	(ii)	(iii)	(iv)
M_1 (GeV)	4.3×10^{12} 8.6×10^{10}	2.6×10^{11} 5.3×10^{9}	5.4×10^{11} 1.1×10^{10}	2.3×10^{12} 4.7×10^{10}
$\tilde{m}_1$ (eV)	0.19 0.11	0.78 0.48	5.17 3.18	1.19 0.7
$Y_B^{\max}$	1.0×10^{-8} 3.6×10^{-10}	1.2×10^{-10} 4.3×10^{-12}	2.8×10^{-11} 9.7×10^{-13}	6.6×10^{-10} 2.3×10^{-11}
Y_B^*	1.3×10^{-10} 2.8×10^{-12}	3.5×10^{-11} 7×10^{-13}	1.2×10^{-12} 2.6×10^{-14}	3.2×10^{-12} 6.9×10^{-14}

we see that fit (i) can accommodate comfortably the observed baryon asymmetry Y_B with phases of $\mathcal{O}(0.1)$ rad, which would not change the LFV predictions. The remaining three models, if the phases are small, would underproduce Y_B. We also note that decreasing the scale M_3 would decrease both Y_B^* and the LFV effects, whereas increasing M_3 to values that would correspond to the perturbative limit for Y_ν would increase Y_B^*, but not

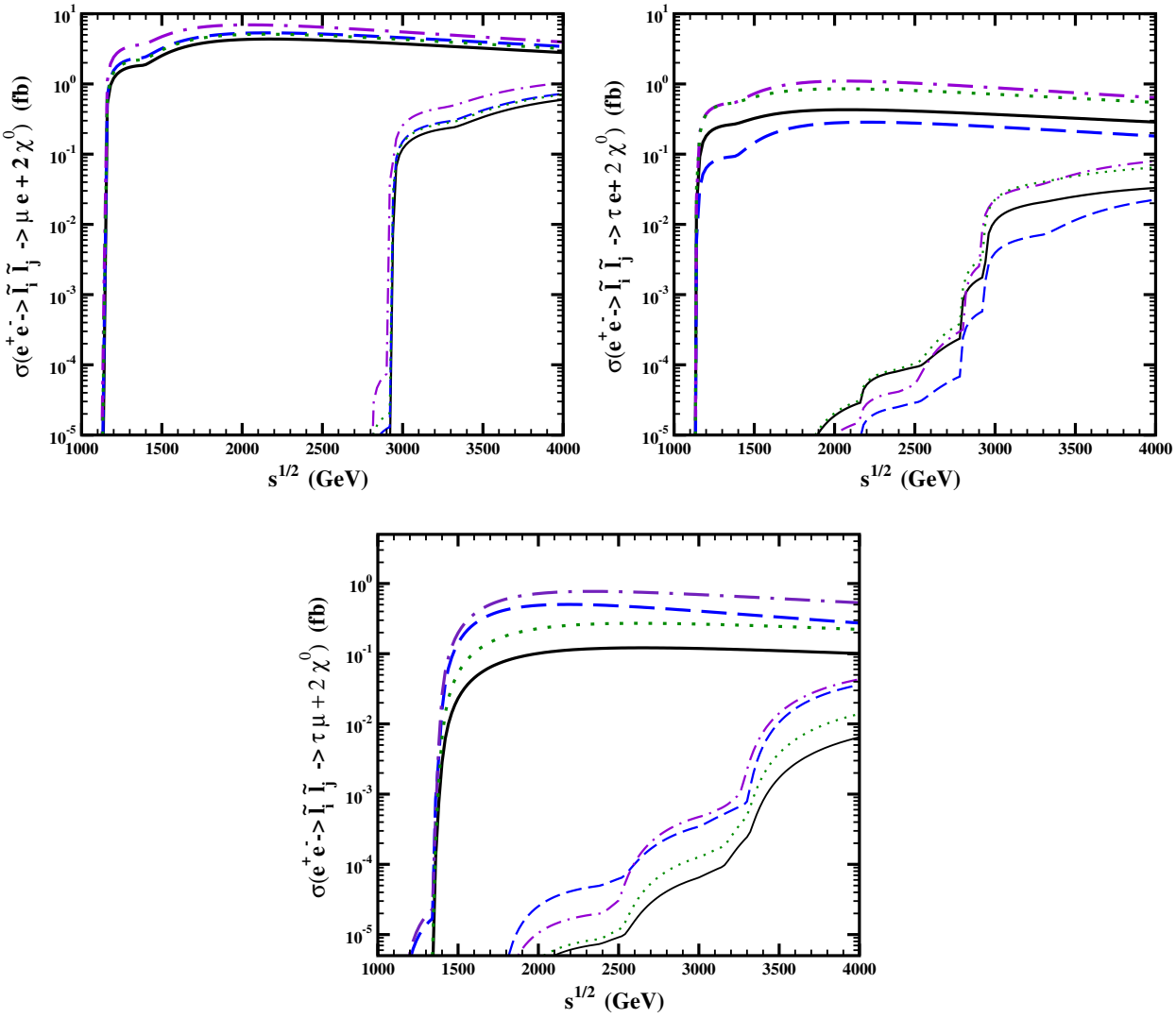

FIG. 4 (color online). Values of the cross sections $\sigma(e^+e^- \to \tilde{\ell}_i^- \tilde{\ell}_j^+ \to \ell_a^\pm \ell_b^\mp + 2\chi^0)$ ($\ell_a \neq \ell_b$ as indicated in each panel) as functions of $\sqrt{s}$. The line styles are the same as those in Fig. 2. For point (a) we use $M_3 = 2 \times 10^{13}$ GeV, while for point (b) we work with $M_3 = 10^{14}$ GeV.

sufficiently to reach its experimental value with small phases.[3] In these cases, either one would have to postulate an additional source of baryon asymmetry, or one should explore predictions for LFV in the presence of large phases. Examining these possibilities lies beyond the scope of this paper. However, we do note that overproduction of baryons is not a problem in our scenario, even in the absence of extra sources of entropy.

V. CONCLUSIONS

Abelian flavor symmetries provide interesting possibilities for understanding the hierarchy of fermion masses and mixing. Despite uncertainties in the choice of $\mathcal{O}(1)$ coefficients, they offer useful insight into physical observables and provide specific predictions for the signals to be expected in various detection channels, which serve as diagnostic tools for discriminating between different models; moreover, several structures predicted by non-Abelian symmetries can be well reproduced by simple Abelian constructions.

In our work, we have explored these possibilities, using updated experimental input from neutrino data, particularly recent measurements of θ_{13}, MEG and the LHC. We have revisited the signatures of charged LFV within an SU(5) GUT framework supplemented by an Abelian flavor symmetry, studying the correlations arising in CMSSM models with parameter values that are favored by the LHC and cosmological considerations, finding interesting possibilities even within this most constrained scenario. Because of their sensitivity to flavor symmetries and model parameters that are not constrained by the neutrino data, particularly those linked to the right-handed neutrino sector, LFV searches may become a powerful tool for distinguishing between different theoretical scenarios.

We first performed a scan of different fits to the neutrino data, selecting representative fits that lead to normal neutrino hierarchies and correlations between the neutrino mixing angles that are compatible with the global analysis of neutrino data in [57]. In doing so, we paid attention to the naturalness of the fit, avoiding artificial cancellations arising from specific choices of coefficients.

We then looked at the expectations for LFV processes in the above models, identifying the range of parameters where observable signatures are possible. In general, fits with similar predictions for the neutrino parameters may lead to different LFV predictions. However, the recent input on θ_{13}, combined with the new MEG bound on $\mu \to e\gamma$ as well as LHC data, does constrain the allowed structures. Further precision in the determination of neutrino parameters could lead to restrictions on the choices of model coefficients but would not constrain the right-handed neutrino charges. New input in this respect, however, could be provided by the rates for LFV processes, since their magnitude is directly linked to these charges, unlike the neutrino mass and mixing parameters. Additional input on the right-handed neutrino sector could be obtained by requiring successful leptogenesis, which in our case can be achieved for a natural choice of parameters.

In the cases we studied, it was possible to establish correlations between the expected rates for radiative LFV decays, the LFV decay of the second lightest neutralino χ_2 at the LHC and LFV in slepton decay at a future LC, for different possibilities for the structure of the heavy Majorana neutrino masses.

Within the CMSSM, the absence of a supersymmetry signal at the LHC data and the discovery of a neutral Higgs weighing $\sim$125 GeV imply that observation of slepton flavor violation at the LHC would be difficult but possible, for points with a lighter spectrum. Observation of LFV at the LC is also possible for the center-of-mass energies above 1 TeV that are compatible with the nominal energies of CLIC. On the other hand, it should be noted here that scenarios less constrained than the CMSSM (which could fit m_h with a lighter sparticle spectrum) might predict observable LFV signals at even smaller energies.

ACKNOWLEDGMENTS

The work of J. E. is supported partly by the London Centre for Terauniverse Studies (LCTS), using funding from the European Research Council via the Advanced Investigator Grant No. 267352. S. L. and M. E. G. thank the CERN Theory Division for its kind hospitality and acknowledges support from the ERC Advanced Investigator Grant No. 267352. The work of M. C. is supported by MultiDark under Grant No. CSD2009-00064 of the Spanish MICINN Consolider-Ingenio 2010 Program. M. E. G. and M. C. acknowledge further support from the MICINN project FPA2011-23781 and Grant No. MICINN-INFN(PG21)AIC-D-2011-0724.

[3]Furthermore, in the case of benchmark point (a) we can see in Fig. 2 that BR($\mu \to e\gamma$) already sets the upper limit of M_3 below 10^{14} GeV.

[1] Y. Fukuda *et al.* (Super-Kamiokande Collaboration), Phys. Rev. Lett. **81**, 1562 (1998).

[2] Y. Fukuda *et al.* (Super-Kamiokande Collaboration), Phys. Rev. Lett. **82**, 1810 (1999); **82**, 2430 (1999); Q. R. Ahmad *et al.* (SNO Collaboration), Phys. Rev. Lett. **87**, 071301 (2001).

[3] K. Eguchi *et al.* (KamLAND Collaboration), Phys. Rev. Lett. **90**, 021802 (2003); T. Araki *et al.* (KamLAND Collaboration), Phys. Rev. Lett. **94**, 081801 (2005).

[4] M. H. Ahn *et al.* (K2K Collaboration), Phys. Rev. Lett. **90**, 041801 (2003).

[5] D. G. Michael *et al.* (MINOS Collaboration), Phys. Rev. Lett. **97**, 191801 (2006).

[6] G. L. Fogli, E. Lisi, A. Marrone, A. Palazzo, and A. M. Rotunno, Phys. Rev. D **84**, 053007 (2011).

[7] M. C. González-García, M. Maltoni, J. Salvado, and T. Schwetz, J. High Energy Phys. 12 (2012) 123.

[8] K. Abe *et al.* (T2K Collaboration), Phys. Rev. Lett. **107**, 041801 (2011).

[9] P. Adamson *et al.* (MINOS Collaboration), Phys. Rev. Lett. **107**, 181802 (2011).

[10] F. P. An *et al.* (Daya Bay Collaboration), Phys. Rev. Lett. **108**, 171803 (2012).

[11] J. K. Ahn *et al.* (RENO Collaboration), Phys. Rev. Lett. **108**, 191802 (2012).

[12] Y. Abe *et al.* (Double Chooz Collaboration), Phys. Lett. B **723**, 66 (2013).

[13] For reviews, see M. Raidal *et al.*, Eur. Phys. J. C **57**, 13 (2008); Y. Kuno and Y. Okada, Rev. Mod. Phys. **73**, 151 (2001).

[14] J. Adam *et al.* (MEG Collaboration), Phys. Rev. Lett. **110**, 201801 (2013).

[15] K. Nakamura (Particle Data Group), J. Phys. G **37**, 075021 (2010).

[16] J. Adam *et al.* (MEG Collaboration), Phys. Rev. Lett. **107**, 171801 (2011).

[17] N. Arkani-Hamed, H. Cheng, J. L. Feng, and L. J. Hall, Phys. Rev. Lett. **77**, 1937 (1996); Nucl. Phys. **B505**, 3 (1997).

[18] J. Hisano, M. M. Nojiri, Y. Shimizu, and M. Tanaka, Phys. Rev. D **60**, 055008 (1999).

[19] M. Guchait, J. Kalinowski, and P. Roy, Eur. Phys. J. C **21**, 163 (2001).

[20] F. Deppisch, J. Kalinowski, H. Päs, A. Redelbach, and R. Rückl, arXiv:hep-ph/0401243, work performed for the LCH study group.

[21] F. Deppisch, H. Päs, A. Redelbach, R. Rückl, and Y. Shimizu, Phys. Rev. D **69**, 054014 (2004).

[22] M. Cannoni, S. Kolb, and O. Panella, Phys. Rev. D **68**, 096002 (2003); M. Cannoni, C. Carimalo, W. Da Silva, and O. Panella, Phys. Rev. D **72**, 115004 (2005); **72**, 119907(E) (2005); M. Cannoni and O. Panella, Phys. Rev. D **79**, 056001 (2009).

[23] E. Carquin, J. Ellis, M. E. Gómez, and S. Lola, J. High Energy Phys. 11 (2011) 050.

[24] A. Abada, A. J. R. Figueiredo, J. C. Romão, and A. M. Teixeira, J. High Energy Phys. 08 (2012) 138.

[25] N. V. Krasnikov, JETP Lett. **65**, 148 (1997); S. I. Bityukov and N. V. Krasnikov, arXiv:hep-ph/9806504; K. Agashe and M. Graesser, Phys. Rev. D **61**, 075008 (2000).

[26] I. Hinchliffe and F. E. Paige, Phys. Rev. D **63**, 115006 (2001).

[27] J. Hisano, R. Kitano, and M. M. Nojiri, Phys. Rev. D **65**, 116002 (2002); D. Carvalho, J. Ellis, M. Gõmez, S. Lola, and J. Romão, Phys. Lett. B **618**, 162 (2005).

[28] A. Bartl, K. Hidaka, K. Hohenwarter-Sodek, T. Kernreiter, W. Majerotto, and W. Porod, Eur. Phys. J. C **46**, 783 (2006).

[29] E. Carquin, J. Ellis, M. E. Gómez, S. Lola, and J. Rodríguez-Quintero, J. High Energy Phys. 05 (2009) 026.

[30] A. Abada, A. J. R. Figueiredo, J. C. Romão, and A. M. Teixeira, J. High Energy Phys. 08 (2011) 099.

[31] J. N. Esteves, J. C. Romão, A. Villanova del Moral, M. Hirsch, J. W. F. Valle, and W. Porod, J. High Energy Phys. 05 (2009) 003.

[32] M. Hirsch, W. Porod, F. Staub, and C. Weiss, Phys. Rev. D **87**, 013010 (2013).

[33] M. Gell-Mann, P. Ramond, and R. Slansky, in *Proceedings of the Stony Brook Supergravity Workshop, New York, 1979*, edited by P. Van Nieuwenhuizen and D. Freedman (North-Holland, Amsterdam, 1979).

[34] F. Borzumati and A. Masiero, Phys. Rev. Lett. **57**, 961 (1986).

[35] J. Hisano, T. Moroi, K. Tobe, and M. Yamaguchi, Phys. Rev. D **53**, 2442 (1996).

[36] M. Gómez, G. Leontaris, S. Lola, and J. Vergados, Phys. Rev. D **59**, 116009 (1999).

[37] J. R. Ellis, M. E. Gómez, G. K. Leontaris, S. Lola, and D. V. Nanopoulos, Eur. Phys. J. C **14**, 319 (2000).

[38] S. Antusch, E. Arganda, M. J. Herrero, and A. M. Teixeira, J. High Energy Phys. 11 (2006) 090.

[39] J. Hisano, D. Nomura, and T. Yanagida, Phys. Lett. B **437**, 351 (1998); W. Buchmüller, D. Delepine, and F. Vissani, Phys. Lett. B **459**, 171 (1999); W. Buchmüller, D. Delepine, and L. T. Handoko, Nucl. Phys. **B576**, 445 (2000); J. L. Feng, Y. Nir, and Y. Shadmi, Phys. Rev. D **61**, 113005 (2000); J. Sato and K. Tobe, Phys. Rev. D **63**, 116010 (2001); J. Hisano and K. Tobe, Phys. Lett. B **510**, 197 (2001); S. Baek, T. Goto, Y. Okada, and K. Okumura, Phys. Rev. D **64**, 095001 (2001); S. Lavignac, I. Masina, and C. A. Savoy, Phys. Lett. B **520**, 269 (2001); D. Carvalho, J. Ellis, M. Gómez, and S. Lola, Phys. Lett. B **515**, 323 (2001); T. Blazek and S. F. King, Phys. Lett. B **518**, 109 (2001).

[40] S. Lola and G. G. Ross, Nucl. Phys. **B553**, 81 (1999).

[41] J. R. Ellis, M. E. Gómez, and S. Lola, J. High Energy Phys. 07 (2007) 052.

[42] For a review, see S. Davidson, E. Nardi, and Y. Nir, Phys. Rep. **466**, 105 (2008); See also M. A. Luty, Phys. Rev. D **45**, 455 (1992); L. Covi, E. Roulet, and F. Vissani, Phys. Lett. B **384**, 169 (1996); W. Buchmuller, P. Di Bari, and M. Plumacher, Ann. Phys. (Amsterdam) **315**, 305 (2005); W. Buchmuller, R. D. Peccei, and T. Yanagida, Annu. Rev. Nucl. Part. Sci. **55**, 311 (2005).

[43] J. R. Ellis and M. Raidal, Nucl. Phys. **B643**, 229 (2002); S. Pascoli, S. T. Petcov, and W. Rodejohann, Phys. Rev. D **68**, 093007 (2003); J. R. Ellis, M. Raidal, and T. Yanagida, Phys. Lett. B **581**, 9 (2004); A. Pilaftsis and T. E. J. Underwood, Nucl. Phys. **B692**, 303 (2004); S. T. Petcov, W. Rodejohann, T. Shindou, and Y. Takanishi, Nucl. Phys. **B739**, 208 (2006).

[44] G. F. Giudice, A. Notari, M. Raidal, A. Riotto, and A. Strumia, Nucl. Phys. **B685**, 89 (2004).
[45] S. Davidson and A. Ibarra, Phys. Lett. B **535**, 25 (2002).
[46] M. E. Gómez, S. Lola, P. Naranjo, and J. Rodríguez-Quintero, J. High Energy Phys. 04 (2009) 043.
[47] See for instance some of the textures studied by G. Altarelli and F. Feruglio, Phys. Lett. B **439**, 112 (1998); J. High Energy Phys. 11 (1998) 021.
[48] G. Altarelli and F. Feruglio, Springer Tracts Mod. Phys. **190**, 169 (2003).
[49] J. Sato and T. Yanagida, Phys. Lett. B **430**, 127 (1998); **493**, 356 (2000).
[50] L. J. Hall, H. Murayama, and N. Weiner, Phys. Rev. Lett. **84**, 2572 (2000).
[51] F. Vissani, J. High Energy Phys. 11 (1998) 025; Phys. Lett. B **508**, 79 (2001).
[52] N. Haba and H. Murayama, Phys. Rev. D **63**, 053010 (2001).
[53] D. Meloni, J. High Energy Phys. 10 (2011) 010.
[54] W. Buchmüller, V. Domcke, and K. Schmitz, J. High Energy Phys. 03 (2012) 008.
[55] G. Altarelli, F. Feruglio, I. Masina, and L. Merlo, J. High Energy Phys. 11 (2012) 139.
[56] J. A. Acosta, A. Aranda, M. A. Buen-Abad, and A. D. Rojas, Phys. Lett. B **718**, 1413 (2013).
[57] G. L. Fogli, E. Lisi, A. Marrone, D. Montanino, A. Palazzo, and A. M. Rotunno, Phys. Rev. D **86**, 013012 (2012).
[58] S. Antusch, J. Kersten, M. Lindner, M. Ratz, and M. A. Schmidt, J. High Energy Phys. 03 (2005) 024.
[59] K. S. Babu, T. Enkhbat, and I. Gogoladze, Nucl. Phys. **B678**, 233 (2004).
[60] K. A. Olive and L. Velasco-Sevilla, J. High Energy Phys. 05 (2008) 052.
[61] G. L. Kane, S. F. King, I. N. R. Peddie, and L. Velasco-Sevilla, J. High Energy Phys. 08 (2005) 083.
[62] G. Altarelli, F. Feruglio, L. Merlo, and E. Stamou, J. High Energy Phys. 08 (2012) 021.
[63] G. Aad *et al.* (ATLAS Collaboration), Phys. Lett. B **716**, 1 (2012).
[64] S. Chatrchyan *et al.* (CMS Collaboration), Phys. Lett. B **716**, 30 (2012).
[65] O. Buchmueller *et al.*, Eur. Phys. J. C **72**, 2243 (2012).
[66] M. Citron, J. Ellis, F. Luo, J. Marrouche, K. A. Olive, and K. J. de Vries, Phys. Rev. D **87**, 036012 (2013).
[67] M. Cannoni, O. Panella, M. Pioppi, and M. Santoni, Phys. Rev. D **86**, 037702 (2012).
[68] J. R. Ellis and S. Lola, Phys. Lett. B **458**, 310 (1999).
[69] J. A. Casas and A. Ibarra, Nucl. Phys. **B618**, 171 (2001).
[70] P. Lebrun *et al.*, arXiv:1209.2543.
[71] M. Battaglia, J.-J. Blaising, J. S. Marshall, M. Thomson, A. Sailer, S. Poss, and E. van der Kraaij, J. High Energy Phys. 09 (2013) 001.
[72] E. Komatsu *et al.* (WMAP Collaboration), Astrophys. J. Suppl. Ser. **192**, 18 (2011).